Journal Article

Synthesis, characterisation and self assembly of biosurfactants based on hydrophobically-modified inulins

Kokubun, S., Ratcliffe, I. and Williams, P.A.

Synthesis, characterisation and self assembly of novel biosurfactants based on hydrophobically-modified inulins

S. Kokubun, I. Ratcliffe and P.A. Williams*

Centre for Water Soluble Polymers, Glyndwr University, Plas Coch, Mold Road, Wrexham, LL11 2AW U.K.

*corresponding author: email williamspa@glyndwr.ac.uk

Keywords

Inulin, critical aggregation concentration, alkenyl succinic anhydrides, dye solubilisation, dynamic light scattering, surface tension

Abstract

Novel biosurfactants have been synthesised using a low energy, environmentally friendly process by the derivatisation of inulin with octenyl (OSA) and dodecenyl (DDSA) succinic anhydrides in aqueous solution. The inulin and its derivatives have been characterised using GPC/MALLS, HPAEC-PAD, FTIR and NMR and the reaction efficiency was found to be between 59-95 %. The efficiency was generally higher for OSA derivatives compared to DDSA derivatives. The hydrophobic derivatives were found to aggregate in solution and the critical aggregation concentration (CAC) was determined using dye solubilisation, surface tension, dynamic light scattering and conductivity. There was reasonable agreement in the CAC values obtained by the different techniques except for conductivity. It was found that the CAC decreased with increasing alkenyl chain length and degree of modification and the values were significantly lower for the DDSA derivatives compared to the OSA derivatives. GPC elution profiles for the DDSA-inulin using 12 mole % reagent confirmed the presence of aggregates with a molecular mass of ~2.5 x 10^6 g/mol and a radius of gyration of ~25 nm corresponding to ~550 inulin molecules. Dynamic light scattering (DLS) study was undertaken to determine the hydrodynamic radius and values obtained for the DDSA (12 %) derivative were 30 nm in both water and 0.1 M sodium nitrate, while for the OSA (12 %) derivative values of 13 nm and 7 nm were obtained. The derivatives have potential application in the stabilisation of particulate dispersions and emulsions and also in the encapsulation and delivery of drugs.

Introduction

Inulin is the second most abundant plant storage polysaccharide after starch and is found in a large number of plants including garlic, leek, banana, chicory and Jerusalem artichoke.[1,2] The main industrial source is chicory roots which contain ~20-25 % inulin on a dry weight basis. Inulin consists of linear chains of β-(2,1) fructose units and typically has a glucose unit attached at the reducing end. The chain length varies with the source but for chicory is

typically between 2-60 fructose units. Inulin is soluble in water but the solubility decreases with increasing polymer chain length.[2] At high inulin concentrations, typically > 15 %, longer chain length molecules form gels on cooling. It has been argued that micron-size crystals are first produced which then associate to form spherical aggregates. These larger aggregates associate further to form three dimensional gel structures.[3,4] Inulin is finding increasing application in food products because of its gelling properties but also because of its nutritional effects, since it is classed as dietary fibre.[5] There is also considerable interest in chemical modification of inulin to form a range of speciality chemicals and recent studies have involved synthesis of hydrophobically modified inulin for potential application as surfactants.[6-10] Modification has largely involved the use of non aqueous solvents, however, Morros et al. [11,12] have recently reported modification of inulin using alkenyl succinic anhydride in water. This reaction has been previously exploited to produce octenyl succinated starches which have wide application as emulsifiers for flavour oil emulsions in the beverage industry.[13-15]

The attachment of the alkyl chains occurs through interaction of the succinic anhydride with the hydroxyl groups on the sugar units. The product is an alkenyl succinate half ester which will carry a negative charge when in the salt form. The reaction is non specific and hence the alkyl chains will attach randomly along the polymer backbone. The overall structure, therefore, will not take on the form of a typical polymeric surfactant in which the hydrophobic groups are attached at one or both ends.[16] Nevertheless, surface tension [7] and interfacial tension [8] studies on octenyl inulin carbamate have shown that the molecules will aggregate at a critical concentration. Surface tension measurements have recently been reported for octenyl succinylated starch and have also indicated that aggregation occurs at a critical concentration.[17,18] The aggregation behaviour of these types of polymer makes them suitable candidates for the dissolution and encapsulation of active compounds. In fact Lu et al. [19] have recently reported the potential application of hydrophobically modified amylopectin micelles in drug delivery.

This study sets out to synthesise a series of hydrophobically modified alkenyl succinylated inulins using octenyl and dodecenyl succinic anhydride at varying degrees of substitution and to gain a fundamental understanding of their aggregation behaviour using a range of techniques.

Materials and methods

Materials

Inulin samples coded Fibruline® DS2 (Degree of Polymerisation, DP > 10) and Inutec N10 were supplied by Cosucra and Beneo Biobased Chemicals respectively and were dried at 70 °C for 24 hours before use.

2-octen-1-yl-succinic anhydride (OSA) and 2-dodecen-1-yl-succinic anhydride (DDSA) were obtained from Aldrich Chemical Co. and were used as received. DMSO-d_6 (99.9 atom % D), Tween 20 (PEG (20) sorbitan monolaurate) and potassium bromide were obtained from Sigma-Aldrich Chemie GmbH. Sudan IV, a water insoluble diazo dye, was obtained from Eastman Kodak Company.

Methods

Synthesis of alkenyl inulin derivatives

All reactions were performed in a 250 mL three-neck round-bottom flask placed in a water bath to maintain a temperature of 25 °C. 30 g of the oven-dried inulin was dispersed in 70 ml of deionised water using propeller mixer (Heidolph Type: ST1 or RZR 50) with PTFE centrifugal stirrer shaft, 6 mm diameter, 400 mm. The pH was adjusted to between 8.30 +/- 0.1 using 1-10 % NaOH solutions using a peristaltic pump (P-1 Pharmacia Fine Chemicals). Various amounts of OSA or DDSA in 10 mL of ethanol [6, 9 and 12 mole %] were added at 25 °C. The modification was carried out until the pH became stable to ensure all OSA or DDSA was consumed, typically ~7 hours. Once the reaction was complete, the resultant product was neutralised with 5 % HCl solution to a pH of 6.0 and was then freeze dried

yielding a white powder. This was purified by Soxhlet extraction for 6 hours using cyclohexane as solvent. Finally, the sample was dried in an oven at 70 °C overnight.

The inulin samples modified using OSA formed optically clear aqueous solutions at room temperature. However, the samples modified with DDSA formed slightly cloudy solutions at room temperature but became clear on heating to 50 °C and remained clear on subsequent cooling.

Characterisation

NMR spectroscopy

5 mg of either native or modified inulin and 0.7 mL of d_6-DMSO were added into a 5 mm thin wall NMR tube and dissolved at 25 °C. H^1 NMR spectra were measured using a 400 MHz magnet at 25 °C. 16 scans were run for all samples. The Pulse Program ZG30 with a 30 degree pulse and a delay of 1 second was used together with Mnova 7.0 software.

FTIR spectroscopy

All samples were dried at 70 °C overnight before analysis. Approximately 1 mg of the sample was milled with approximately 100 mg of dried KBr using an agate mortar and pestle for several minutes until fully mixed to form a very fine powder. The powder was then compressed into a thin transparent KBr pellet using a 15 Ton Manual Press and a P/N 03000 13 mm pellet die (Max load 10.0 Tons) from Specac Limited. FTIR spectra were recorded using a Perkin-Elmer FTIR spectrometer spectrum RX 1. 16 scans were performed between 400 and 4000 cm^{-1}. Spectral analysis and display were performed using the interactive Perkin-Elmer Read.IR3 version 3.0 software.

Gel permeation chromatography

The molecular mass distributions of the native and modified inulin samples were determined using gel permeation chromatography (GPC). The GPC system consisted of a Suprema column (dimensions 300 mm x 8 mm; Polymer Standards Service GmbH) with 10 micron

126 beads with a 100 Å pore size, protected by a guard column (Polymer Standards Service
127 GmbH: 10 microns).The eluent used was 0.1 M sodium nitrate containing 0.005 % sodium
128 azide and was filtered with a GSWP 0.45 µm filter (Millipore) and degassed (Vacuum
129 degasser CS 1615/Cambridge Scientific Instrument, Ltd) before use. The samples (0.2-
130 1.0 %) were dissolved in the eluent at 50 °C for two hours and left tumbling overnight at 25
131 °C to fully dissolve. The flow rate was set at 0.5 mL per minute using a Waters Corporation
132 515 HPLC pump and the loop volume was 200 or 1000 µL (Rheodyne model: 7125). A
133 Dawn® DSP Laser Photometer and OPTILAB DSP Interferometric Refractometer (Wyatt
134 Technology Corporation) were used as detectors. The samples were passed through a 0.45
135 µm pore size nylon syringe filter before being injected onto the columns. Measurements
136 were performed in duplicate. The molecular weight was determined using a designated
137 software Astra for Windows 4.90.08 QELSS 2.XX. The Debye model was used for all
138 evaluation analyses. The refractive index increment (dn/dc) of the native inulin was
139 determined in the eluent and found to be 0.131 mL/g in agreement with the literature value
140 [20]. The dn/dc values were also determined for the OSA (12 %)-inulin and DDSA (12 %)-inulin
141 samples and found to be 0.096 and 0.121 mL/g respectively.
142
143 *High-Performance Anion-Exchange Chromatography (HPAEC)*
144 Inulin N10 was dissolved in deionised water (200 mg/ml) and filtered through a 0.45 µm
145 nylon membrane. Injections of 25 µl were analysed by Dionex^{R} High Performance Anion
146 Exchange Chromatography and Pulsed Amperometric Detection (HPAEC-PAD) as
147 described elsewhere [21] except that the PA 100 column was operated at 35 °C using a
148 discontinuous gradient of sodium acetate as follows: 0.0 M (0-2 min) 0.0-0.5 M (2-40 min)
149 0.5-1.0 M (40-45 min), 1.0-0.0 M (45-48 min) and 0.0 M (48-50 min) .
150
151 ***Critical aggregation concentration (CAC)***
152 *Dye solubilisation*

153 The CAC was determined by the dye solubilisation technique using Sudan IV. 10 mg of the
154 dye was added to 10 ml of the native inulin, ASA-inulins or Tween 20 at varying
155 concentration in deionised water and in the presence of 0.1 M of sodium nitrate solution. The
156 samples were mixed at 40 °C overnight and filtered using a Millex-GP 0.22 µm filter
157 (Millipore Ireland Ltd) into disposable UV grade 10 mm path length cuvettes (CXA-110-0053
158 from Fisher Scientific Ltd). The absorbance of the solutions was measured at 510 nm using
159 a Lambda 25 UV/VIS Spectrometer PerkinElmer. Measurements were performed in
160 duplicate. The CAC was determined from the increase in absorbance.
161
162 *Dynamic light scattering*
163 The dynamic light scattering measurements were performed at 25 ˚C using a Zetasizer Nano
164 ZS (Malvem Instrument Lab, Malvern, UK) optical system equipped with a 5 m_w He-Ne laser
165 (λ_0 633 nm) and a digital correlator. The scattering intensity was measured at an angle of
166 175° to the incident beam. The analysis was performed using disposable UV grade 10 mm
167 path length cuvettes (CXA-110-0053, Fisher Scientific Ltd), cleaned with compressed air
168 several times before use. Experimental solutions samples were prepared by diluting a 4 %
169 w/w of stock with either deionised water or 0.1 M sodium nitrate solution and were filtered
170 through a Millex-GP 0.22 µm filter (Millipore Ireland Ltd) directly into the cuvette. 15 runs
171 were performed for each sample, equilibration time was 2 hours. Zetasizer Software 6.20 ©
172 2002-2010 Malvern Instruments Ltd was used for data analysis. The CAC was determined
173 from the change in the slope of the plot of the intensity of scattered light as a function of
174 concentration. The hydrodynamic diameter of the aggregates was obtained from the Stokes-
175 Einstein relationship using the instrument software.
176
177 *Conductivity*
178 Conductivity measurements were carried out at 25 ˚C ± 1 ˚C using a Jenway 4010
179 conductivity meter with a cell constant of 1.00 cm^{-1}. The conductivity meter was calibrated
180 using 0.01 M KCl solution which gave a value of 1413 µs cm^{-1} at 25 °C in agreement with

the literature [22]. All samples were prepared at varying concentration using deionised water with a conductivity of < 0.02 μs cm^{-1}.

Surface tension

The surface tension of modified inulin solutions at varying concentration was measured at 25 °C ± 1 °C using the Du Nouy ring method with a Tensiometer K8 and a 4 cm circumference platinum ring RI 01 from Krüss GmbH. Measurements were performed in triplicate. The equilibrium surface tension was plotted as a function of modified inulin concentration and the CAC was estimated from the change in slope of the plot. It was not possible to determine the dynamic surface tension due to sample foaming.

Results and discussion

Characterisation

NMR spectroscopy

^{1}H NMR spectra of the native and two modified inulin samples are given in Figure 1a,1b and 1c respectively. The prominent peaks at 2.54 ppm and 3.34 ppm are from the solvent i.e. DMSO and HDO respectively and the peaks from 3.14 ppm to 5.16 ppm peaks are from the inulin itself (Figure 1a). ^{1}H NMR signals at 0.85 ppm, 1.26 ppm and 1.94 ppm [23,24] correspond to the methyl and methylene groups of OSA and DDSA (Figure 1b and 1c). The amount of alkenyl chains incorporated was calculated from the ratio of the area of the peak at 0.85 ppm to the area of the peaks from 3.14-5.16 ppm from inulin and the results are presented in Table 1. The reaction efficiency was generally higher for the OSA derivatives compared to the DDSA derivatives. Interestingly, the reaction efficiency improved markedly for DDSA when the reaction was performed at 50 °C and this is attributed to the improved miscibility of DDSA with water.

FTIR spectroscopy

208 FTIR spectra of the native and modified inulin samples are presented in Figure 2. The peaks
209 for the native inulin at 3380 cm^{-1}, 2931 cm^{-1} and 1030 cm^{-1} indicate O–H stretching, CH_2
210 stretching and C–O–C bending respectively.[25] The spectra of both OSA-inulin and DDSA-
211 inulin show two new peaks at 1571 cm^{-1} and 1724 cm^{-1} due to the formation of the ester
212 linkage. The peaks are assigned to asymmetric COO^- stretching and ester carbonyl
213 stretching respectively.[24] It has previously been reported that the CH_2 stretching band at
214 2928 cm^{-1} increased after modification of starches because of the contribution from the
215 carbon chain associated with the alkenyl succinic group.[26] However the CH_2 stretching band
216 at 2931 cm^{-1} for our modified inulins were not comparably enhanced.
217
218 *Gel permeation chromatography*
219 The RI elution profiles of the native, OSA (12 %)-inulin and DDSA (12 %)-inulin samples
220 using varying injection concentrations are given in Figures 3a and 3b. The weight average,
221 M_w, and number average, M_n, molecular mass values are presented in Table 2. The M_w
222 value obtained for the unmodified DS2 sample was ~3,760 g/mol which is equivalent to ~23
223 fructose units and is about twice the value expected from the manufacturers' specifications.
224 The Inutec N10 sample was found to be slightly more polydisperse than the Fibruline DS2
225 sample and showed a small secondary peak eluting at an elution volume of ~11 mL (data
226 not shown). The OSA (12 %)-inulin elutes earlier than the native inulin corresponding to an
227 increased molecular mass and there is a small peak at high elution volume (~11.2 mL) which
228 is perhaps evidence of some depolymerisation. The M_w values obtained using injection
229 concentrations of 0.2 % and 0.4 % were slightly higher than those of the native inulin and
230 close to the theoretical value expected of ~4,200 g/mol. However, when the injection
231 concentration was increased to 1 % a higher value was obtained (5,460 g/mol) which may
232 be due to the presence of polymer aggregates. In the case of DDSA (12%)-inulin a similar
233 shift in the main peak to the high molecular mass side was observed together with a small
234 peak at an elution volume of ~11.2 mL attributed above to depolymerisation. In addition,

however, another peak was observed at an elution volume of 6-8 mL which is attributed to micellar-like aggregates. The molecular mass of the high molecular mass peak is ~2.5 x 10^6 g/mol which suggests that the aggregates consist of ~550 molecules. Analysis of the light scattering data indicated that the radius of gyration of the aggregates was of the order of ~25 nm.

HPAEC-PAD

The HPAEC elution profile for the native inulin sample is presented in Figure 4 together with a calibration curve. The individual peaks with elution times of ~8-18 mins correspond to inulin molecules with DP values of 2-10. The results show, therefore, that a significant amount of material is present with DP 10-50 which is in agreement with the GPC data reported above.

Critical aggregation concentration

Dye solubilisation

The absorbances obtained for native inulin, OSA (12 %)- and DDSA (12 %)-inulins in the presence and absence of electrolyte are given in Figure 5 together with data obtained for Tween 20 as a comparison. The absorbance for the native inulin does not change over the concentration range studied, as expected, confirming that there is no interaction with the dye. For the ASA-inulin samples and the Tween 20 the absorbance values increase significantly above a certain critical concentration which is indicative of the formation of aggregates. For the Tween 20 the increase in absorbance occurs at ~ 0.005 % concentration which is the same value reported by Patist et al. who also measured the CAC using dye solubilisation.[27] The CAC values for all the samples are summarised in Table 3. It is noted that for DDSA-inulin the CAC decreases as the amount of hydrophobe increases. The CAC for the DDSA-inulin was found to be 0.02-0.20% as the DDSA content decreased from 12 to 6% while for OSA-inulin the value was 0.8 % for all of the samples.

It is interesting to note that, despite the fact that the ASA-inulins are negatively charged, the CAC does not appear to change to any great extent in the presence of electrolyte which is contrary to the behaviour of simple ionic surfactants. For the latter systems the critical micelle concentration, CMC, decreases as the ionic strength increases since the electrolyte will screen the repulsions between the ionic head groups as the surfactant molecules pack together thus promoting micelle formation. In the case of the ASA-inulins, the hydrophobic chains are attached randomly along the inulin chain, and hence it is not expected that the molecules will aggregate to form discrete spherical structures. The fact that the ASA-inulin CAC is not sensitive to the presence of electrolyte indicates that the charged groups are not packed close together.

Dynamic light scattering

The scattering intensity of solutions of the OSA- and DDSA-inulin samples are plotted as a function of concentration in Figure 6. An inflection, which is attributed to the CAC, is observed for the OSA-inulins at a concentration of ~0.7 % -0.9 % and for DDSA-inulins at a concentration of 0.02 % -0.05 %. These values are in reasonable agreement with the CAC values obtained by dye solubilisation. Figure 7 is a plot of the Z- average hydrodynamic radius, R_h, of the modified samples as a function of concentration as determined by dynamic light scattering. For the DDSA (12 %)-inulin the radius for the aggregates was found to be ~30 nm in both water and 0.1 M sodium nitrate. This value is of the order found for R_g by light scattering as reported above. For the OSA-inulin samples R_h for the aggregates was found to be 13 nm in water and 7 nm in 0.1 M sodium nitrate.

Conductivity

It is well known that for simple ionic surfactants that there is a change in the slope of the plot of conductivity against concentration at the critical micelle concentration. The inflection is a result of the fact that upon micellisation the charged head-groups pack close together and counterion condensation occurs to reduce charge repulsions. The conductivity of solutions of

DDSA-inulin at varying levels of hydrophobe incorporation are shown in Figure 8 as a function of concentration. There is no clear inflection observed which is consistent with the observations above confirming that the head groups do not pack close together. Similar findings were observed for the OSA-inulins (data not shown). Interestingly, Krstonosic et al. (2011) performed conductivity experiments on OSA-starch and observed an inflection.[18]

Surface tension

The surface tension of OSA-inulin and DDSA-inulin samples are plotted as a function of concentration in Figure 9. The inflection in the curves which corresponds to the CAC occurs at concentrations of 0.6 % and 0.05 % respectively. These values are in good agreement with values reported from dye solublisation and dynamic light scattering data above (Table 3). The surface tension was found to be ~35-40 mN/m at the CAC. Stevens et al. reported a similar value for an octyl carbamate inulin derivative which was found to have a CAC ~0.01 %. [6,7]

Figure 10 provides an overall summary of the CAC values of the samples as a function of % hydrophobe incorporation and demonstrates that there is reasonable agreement for the values obtained using the various techniques.

Conclusions

Inulin can be readily modified using alkylene succinic anhydrides in aqueous solution and the reaction efficiency is higher for OSA compared to DDSA derivatives. The products behave as surfactants and are able to associate in solution to form aggregates. The CAC is dependent on the length and number of the alkenyl chains and for the DDSA (12 %)-inulin the CAC values are an order of magnitude lower than for the OSA derivatives. The DDSA aggregates have been shown to consist of ~550 molecules with a radius of gyration of ~25 nm and R_h ~30 nm. Smaller aggregates (7-13 nm) were obtained for OSA-inulin.

Acknowledgments

The authors gratefully acknowledge experimental support for HPAEC-PAD from Dr Andy Cairns from the Institute of Biological, Environmental and Rural Sciences (IBERS), Aberystwyth University and Department of Chemistry, Bangor for NMR. The work has been sponsored by the BBSRC Integrated Biorefining Research and Technology (IBTI) Club [Grant Reference Number BB/1005315/1].

References

(1) Franck, A., *In Food Polysaccharides and their applications*, 2nd ed.; Stephens, A.M., Phillips, G.O., Williams, P.A., Eds.; Taylor and Francis group, Florida, USA , 2006; p 335-351.

(2) Meyer, D. In *Handbook of hydrocolloids*, 2nd ed.; Phillips, G.O., Williams, P.A., Eds.; Woodhead Publishing Ltd: Cambridge, UK, 2009; p 829-848.

(3) Bot, A.; Erle, U.; Vreeker, R.; Agterof, G.M. *Food hydrocolloids* **2004**, 18, 547-556.

(4) Glibowski, P.; Pikus, S. *Carbohydr. Polym.* **2011**, 83, 635-639.

(5) Meyer, D.; Bayarri, S.; Tarrega, A.; Costell, E. *Food Hydrocolloids* **2011**, 25, 1881-1890.

(6) Stevens, C.V.; Meriggi, A.; Booten, K. *Biomacromolecules* **2001**, 2, 1-16.

(7) Stevens, C.V.; Meriggi, A.; Peristeropoulou, M.; Christov, P.P.; Booten, K.; Levecke, B.; Vandamme, A.; Pittevils, N; Tadros, T. F. *Biomacromolecules* **2001**, 2, 21256-1259.

(8) Exerowa, D.; Gotchev, G.; Kolarov, T.; Kristov, K.; Levecke, B.; Tadros, T. F. *Colloids Surf., A* **2009**, 334, 87-91.

(9) Khristov, K.; Czarnecki, J. *Curr. Opin. Colloid and Interface Sci.* **2010**, 15, 324-329.

(10) Gochev, G.; Petkova, H.; Kolarov, T.; Khristov, K.; Levecke, B.; Tadros, T. F.; Exerowa, D. *Colloids Surf., A* **2011**, 391, 101-104.

(11) Morros, J.; Levecke, B.; Rosa I.M. *Carbohydr. Polym.* **2010**, 81, 681-686.

(12) Morros, J.; Levecke, B.; Rosa I.M. *Carbohydr. Polym.* **2011**, 84, 1110-1116.

345 (13) Wurzburg, O. T., In *Food Polysaccharides and their applications*, 2nd ed.; Stephens,
346 A.M., Phillips, G.O., Williams, P.A., Eds.; Taylor and Francis group, Florida, USA , 2006, p
347 87-118.
348 (14) Bai, Y.; Shi, Y.C. *Carbohydr. Polym.* **2011**, 83, 520-527.
349 (15) Segura, C.M.; Chel, G.L.; Betancur, A.D. *Food Hydrocolloids* **2008**, 22, 1467-1474.
350 (16) Kristov, K.; Czarnecki, J. *Curr. Opin. Colloid and Interface Sci.* **2010**, 15, 324-329.
351 (17) Varona, S.; Martin, A.; Cocero, M.J. *Chem. Eng. Process.* **2009**, 48, 1121-1128
352 (18) Krstonsic, V.; Dokic, L.; Milanovic, J. *Food Hydrocolloids* **2011**, 25, 361-367.
353 (19) Lu, H.W.; Zhang, L.M.; Wang, C.; Chen, R.F. *Carbohydr. Polym.* **2011**, 83, 1499-1506.
354 (20) Dorine, L. V.; Joop, A. P.; Jan, G. B.; Herman, V. B. *Carbohydr. Res.***1995**, 271, 1, 101-
355 112.
356 (21) Cairns, A. J.; Nash. R.; Machado De Carvalho, M. A.; Sims, I. M. *New Phytol.* **1999**,
357 142, 79-91.
358 (22) Wu,T.Y.; Su, S.G.; Lin,Y.C.; Wang, H.P.; Lin, M.W.; Gung,S.T.; Sun,W.I. *Electrochim.*
359 *Acta* **2010**, 56, 2, 853-862.
360 (23) Tizzotti, M.J.; Sweedman, M.C.; Tang. D.; Schaefer, C.; Gilbert, G. R. *J. Agric. Food*
361 *Chem.* **2011**, 59, 6913-6919.
362 (24) Chi, H.; Xu, K.; Xue, D.; Song, C.; Zhang, W.; Wang, P. *Food Res. Int.* **2007**, 40, 232-
363 238.
364 (25) Fares, M.M.; Salem, M.S.; Khanfar, M. *Int. J. Pharm.* **2011**, 410, 1-2, 206-211.
365 (26) Bai, Y.; Shi, Y.C.; Wetzel, D.L. *J. Agric. Food Chem.* **2009**, 57, 6443-6448.
366 (27) Patist, A.; Bhagwat, S.S.; Penfield, K.W.; Aikens, P.; Shah, D.O. *J. Surfactants Deterg.*
367 **2000**, 3, 1, 53-58.
368
369
370

371 **List of Figures**

372

373 **Figure 1.** ^{1}H NMR spectra of (a) native inulin DS2 (b) OSA(12 %)-inulin (c) DDSA(12 %)-
374 inulin

375

376 **Figure 2**. FTIR spectra of native inulin, OSA-inulin and DDSA-inulin

377

378 **Figure 3.** GPC RI elution profiles for native inulin and (a) OSA(12 %)-inulin (b) DDSA (12
379 %)-inulin at varying injection concentrations

380

381 **Figure 4**. HPAEC-PAD chromatographic elution profile of the native inulin N10

382

383 **Figure 5**. Concentration dependence of the UV-vis absorbance of Tween 20 and ASA-
384 inulins in presence of excess Sudan IV

385

386 **Figure 6.** Scattering intensity of ASA-inulin samples as a function of concentration obtained
387 by dynamic light scattering

388

389 **Figure 7.** Hydrodynamic diameter of ASA-inulin samples as a function of concentration

390

391 **Figure 8.** Concentration dependence of conductivity of DDSA-inulins as a function of
392 concentration

393

394 **Figure 9.** Concentration dependence of the surface tension of DDSA (12 %)-inulin and OSA
395 (12 %)-inulin samples as a function of concentration

396

Figure 10. Comparison of the CAC values for ASA-inulin samples with varying % hydrophobe incorporation using dye solubilisation, dynamic light scattering and surface tension measurements

Table 1. Effect of ASA concentrations on the DS and reaction efficiencies of ASA-inulins

Table 2. Molecular mass and polydispersity of the inulin and ASA-inulin samples

Table 3. Critical aggregation concentrations of the ASA-inulin samples using various techniques

(a)

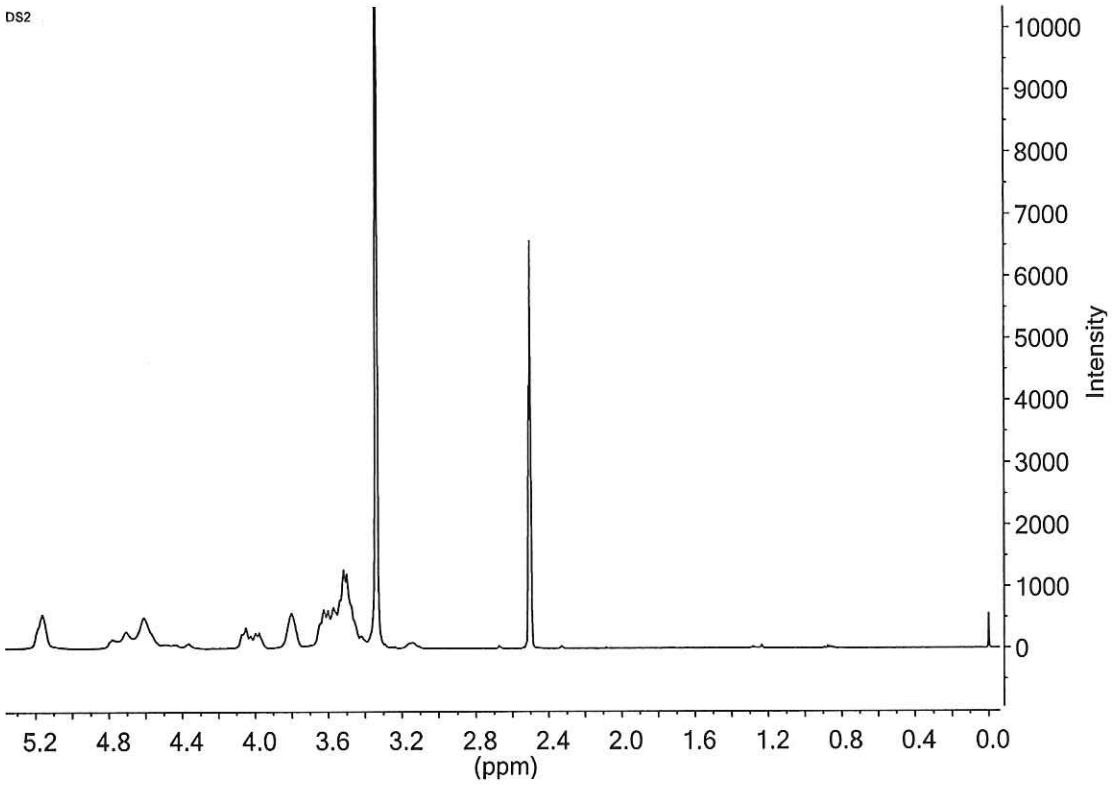
DS2
10000
9000
8000
7000
6000
5000
4000
3000
2000
1000
0
Intensity
5.2
4.8
4.4
4.0
3.6
3.2
2.8
2.4
2.0
1.6
1.2
0.8
0.4
0.0
(ppm)

(b)

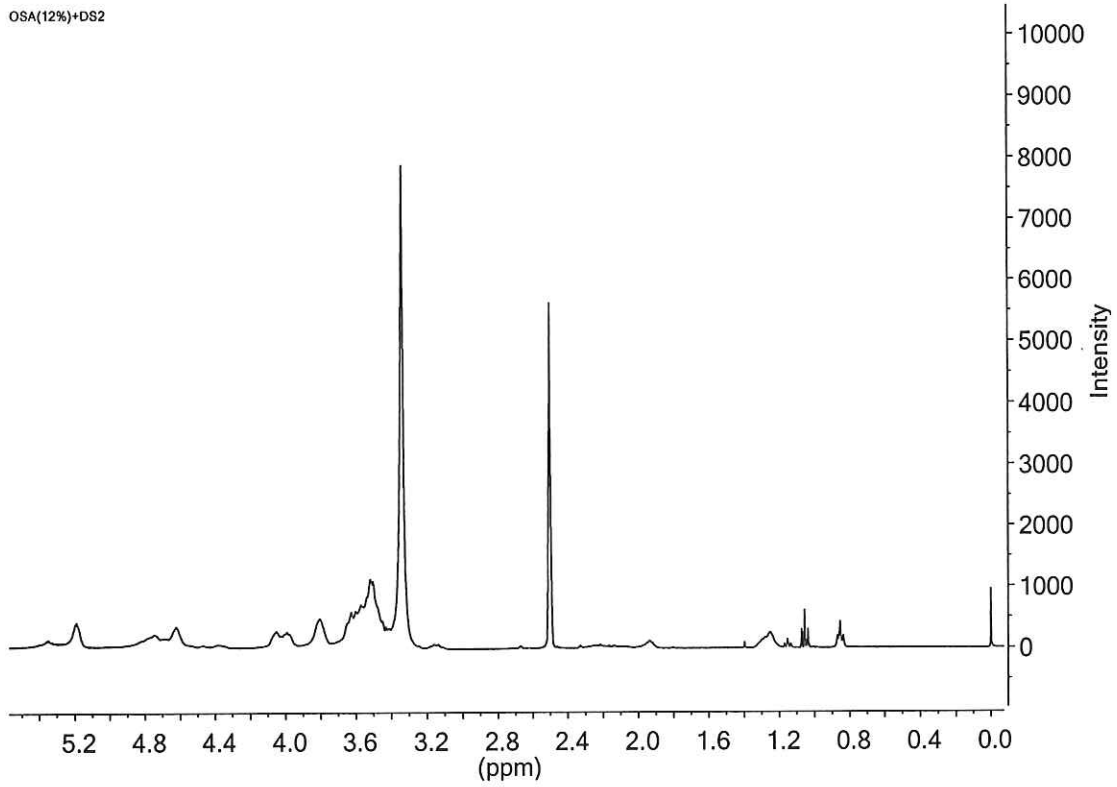
OSA(12%)+DS2
10000
9000
8000
7000
6000
5000
4000
3000
2000
1000
0
Intensity
5.2
4.8
4.4
4.0
3.6
3.2
2.8
2.4
2.0
1.6
1.2
0.8
0.4
0.0
(ppm)

(c)

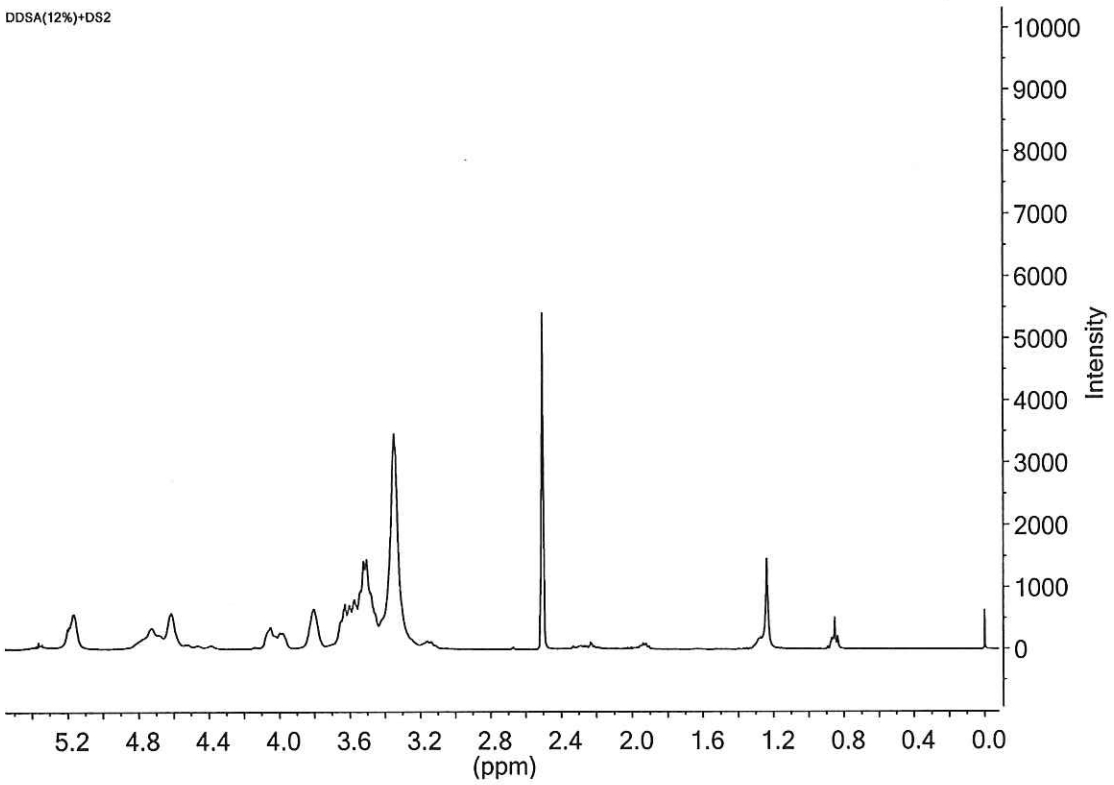

Figure 1. ^{1}H NMR spectra of (a) native inulin DS2 (b) OSA(12 %)-inulin (c) DDSA(12 %)-inulin

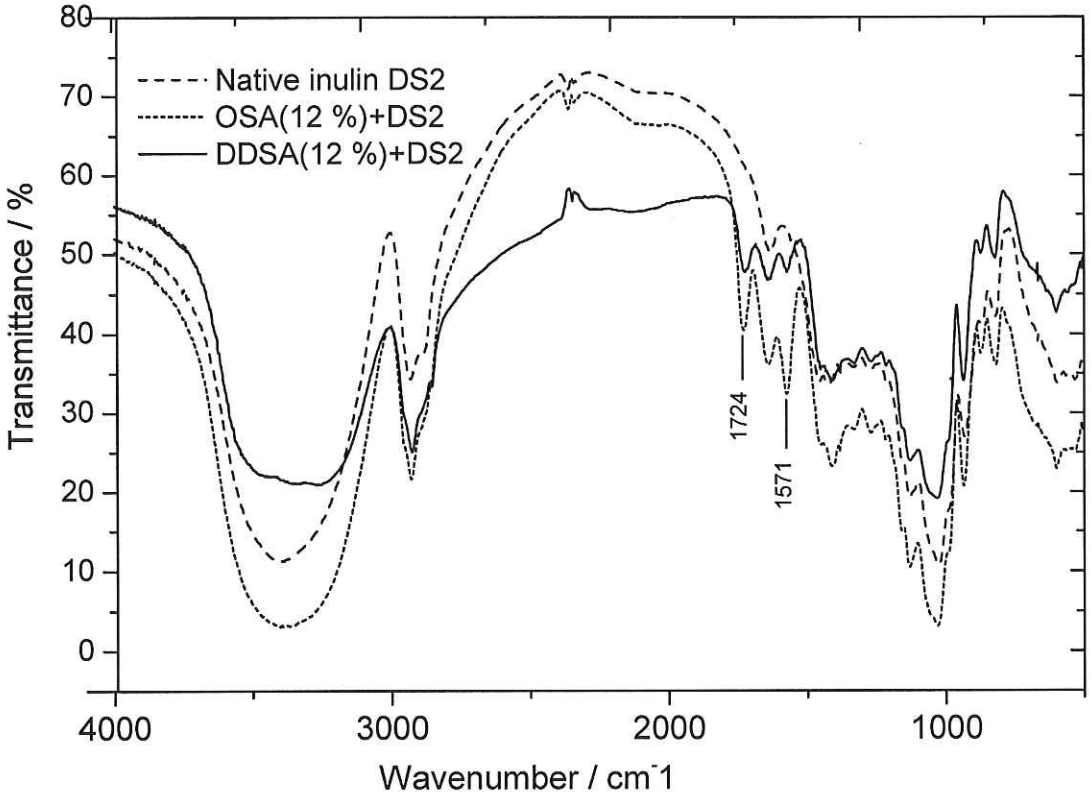

Figure 2. FT-IR spectra of native inulin, OSA-inulin and DDSA-inulin.

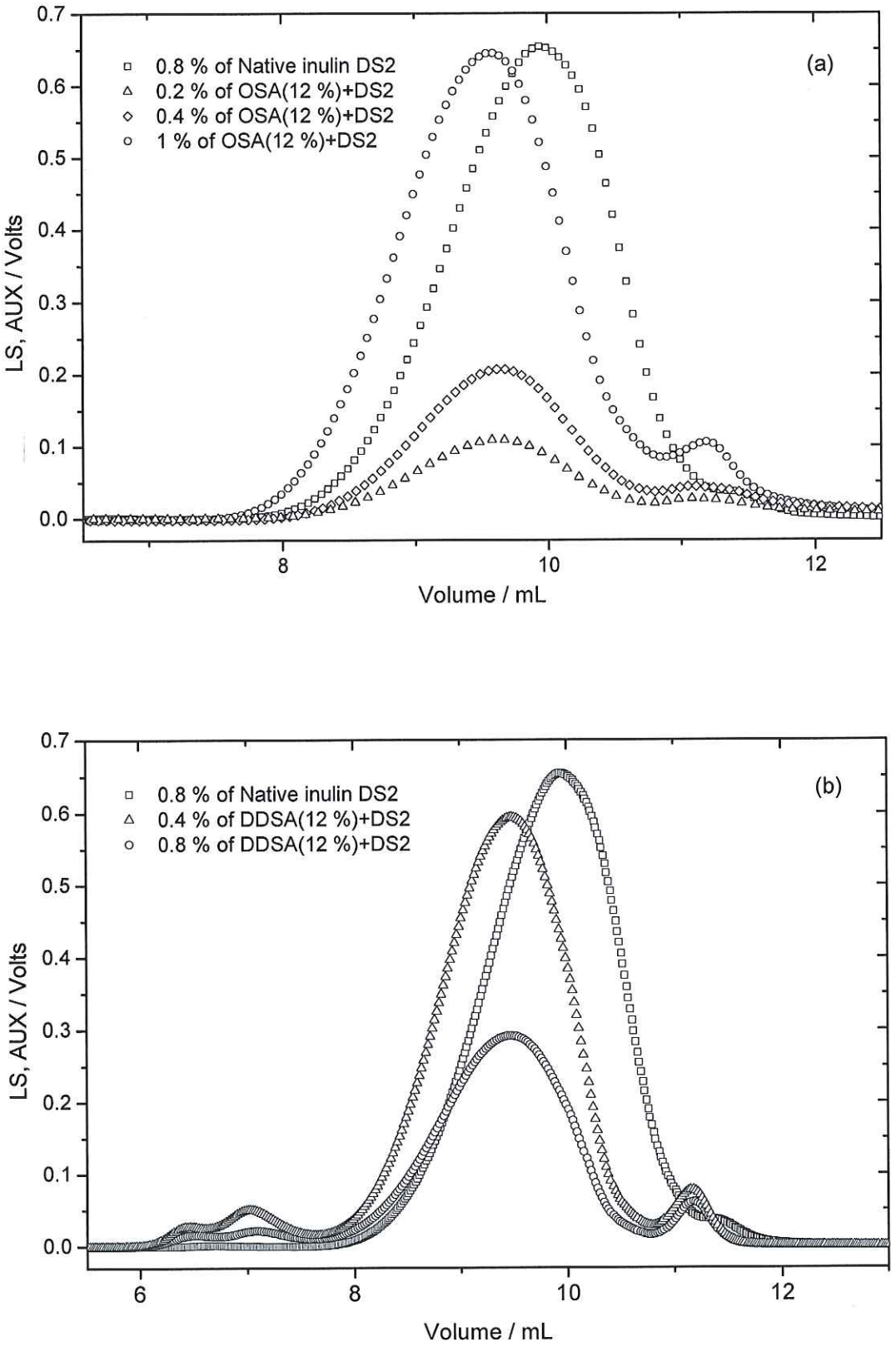

Figure 3. GPC RI elution profiles for native inulin and (a) OSA(12 %)-inulin (b) DDSA (12 %)-inulin at varying injection concentrations

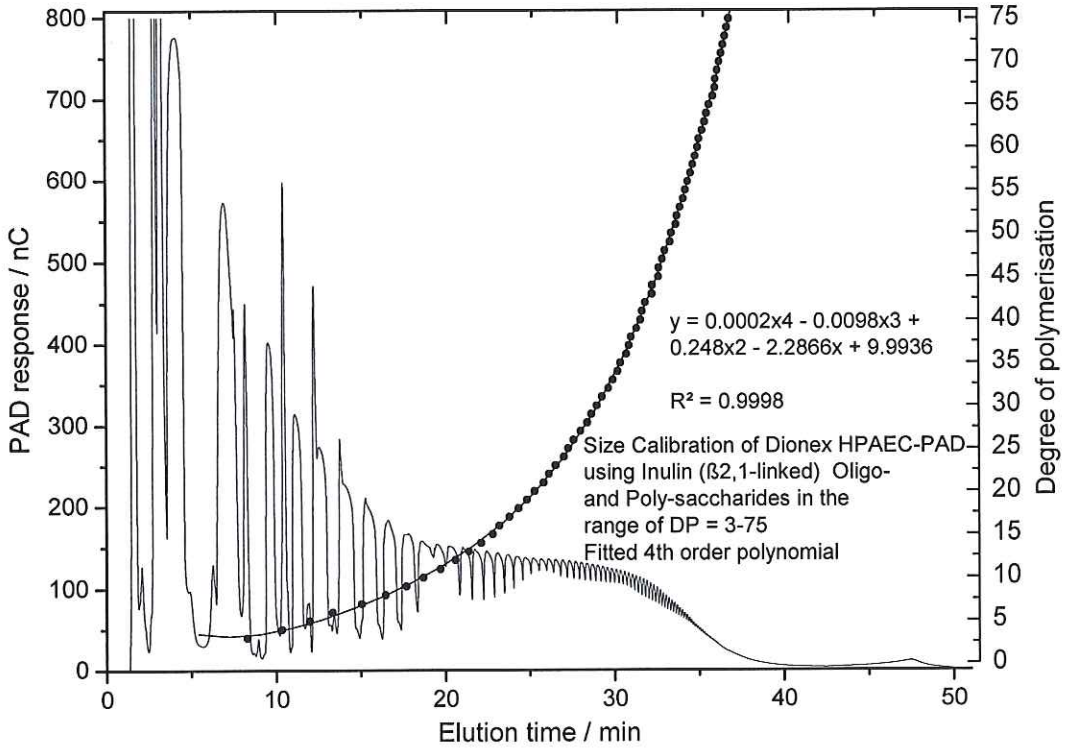

Figure 4. HPAEC-PAD chromatographic elution profile of the native inulin N10

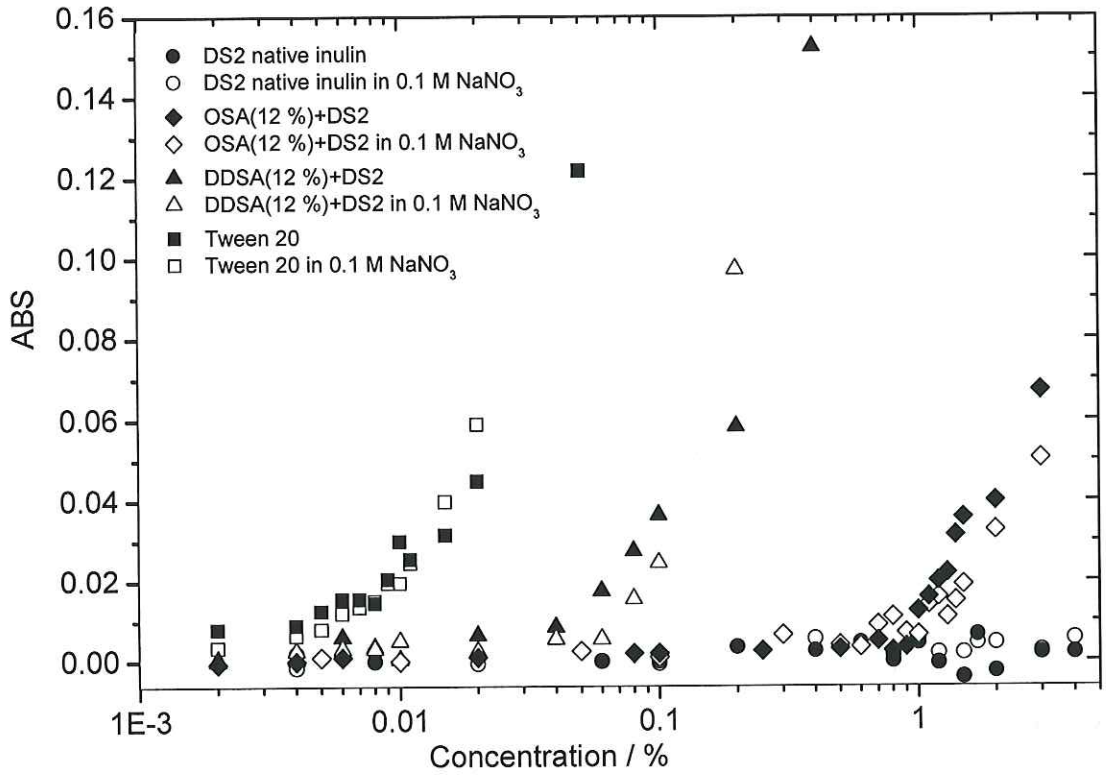

Figure 5. Concentration dependence of the UV-vis absorbance of Tween 20 and ASA-inulins in presence of excess Sudan IV.

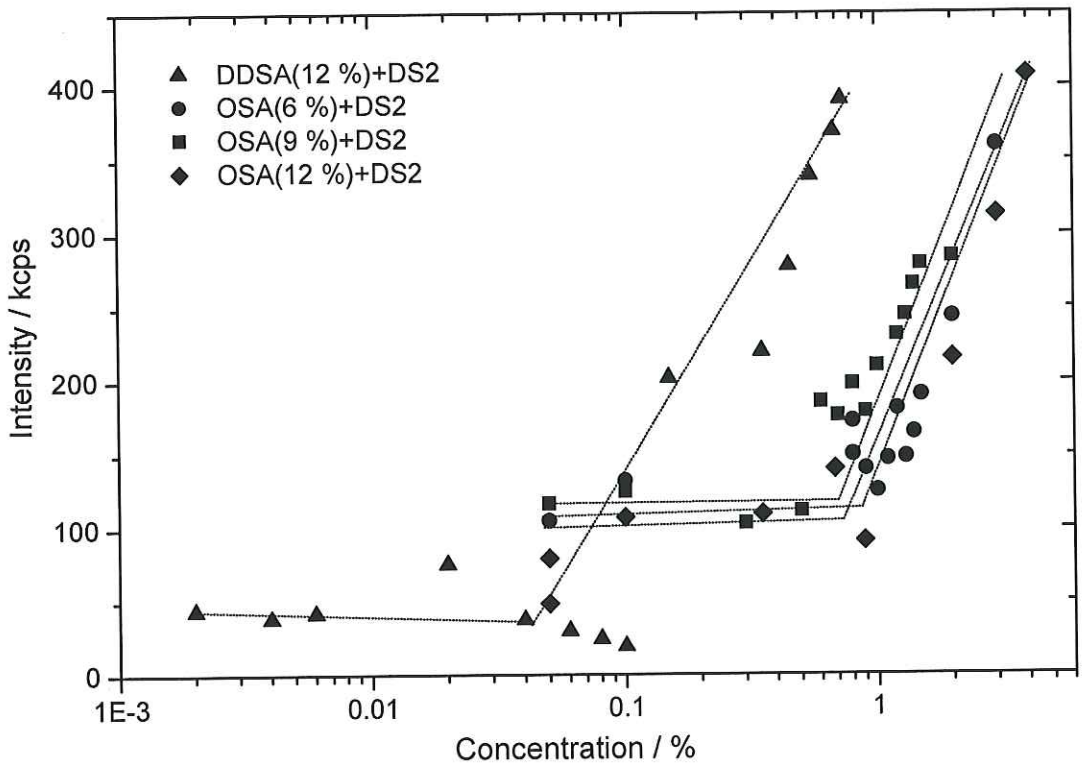

Figure 6. Scattering intensity of ASA-inulin samples as a function of concentration obtained by dynamic light scattering.

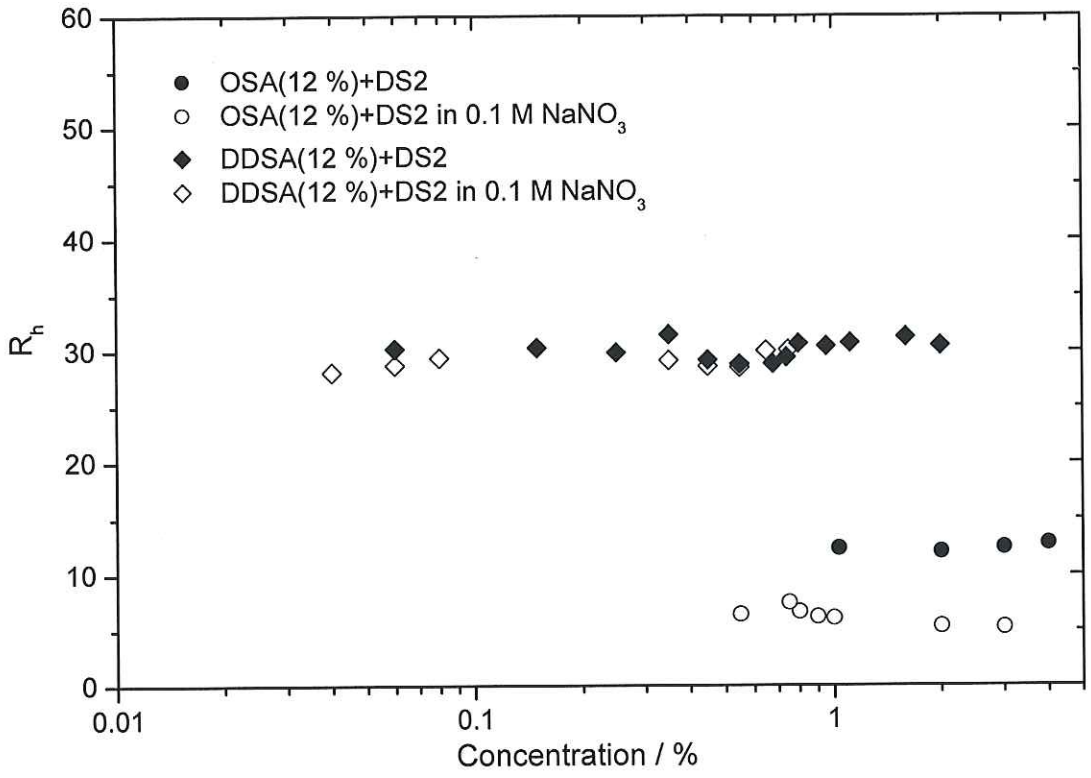

Figure 7. Hydrodynamic diameter of ASA-inulin samples as a function of concentration.

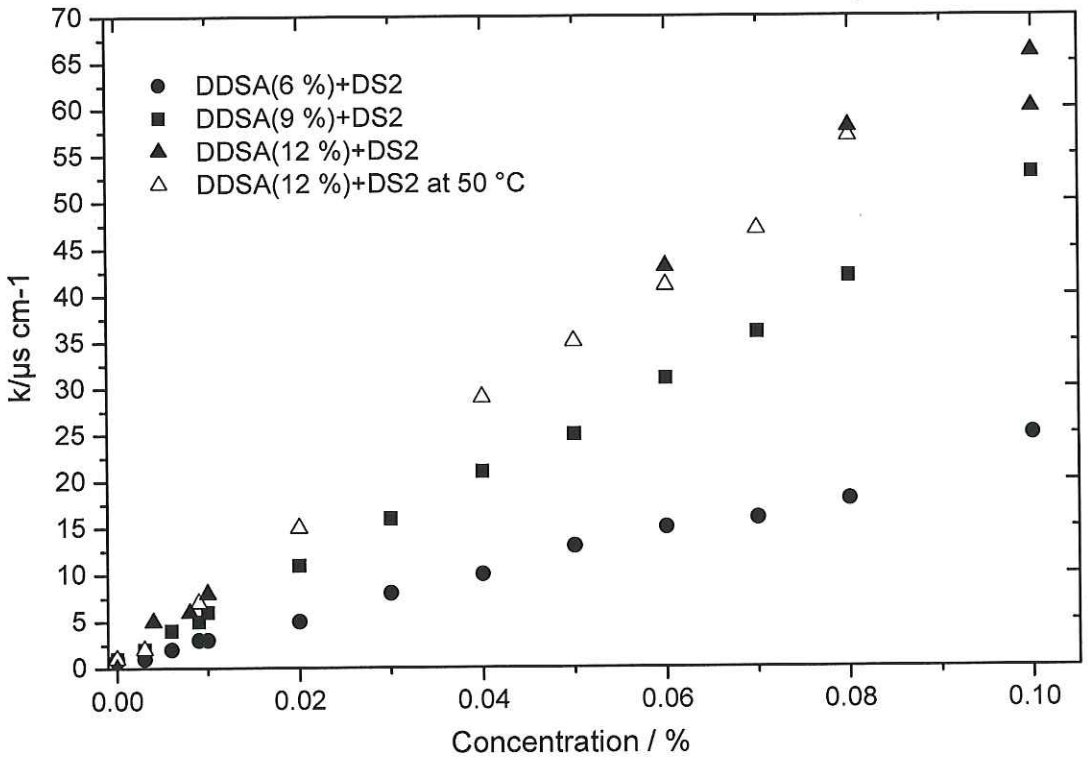

Figure 8. Concentration dependence of conductivity of DDSA-inulins as a function of concentration.

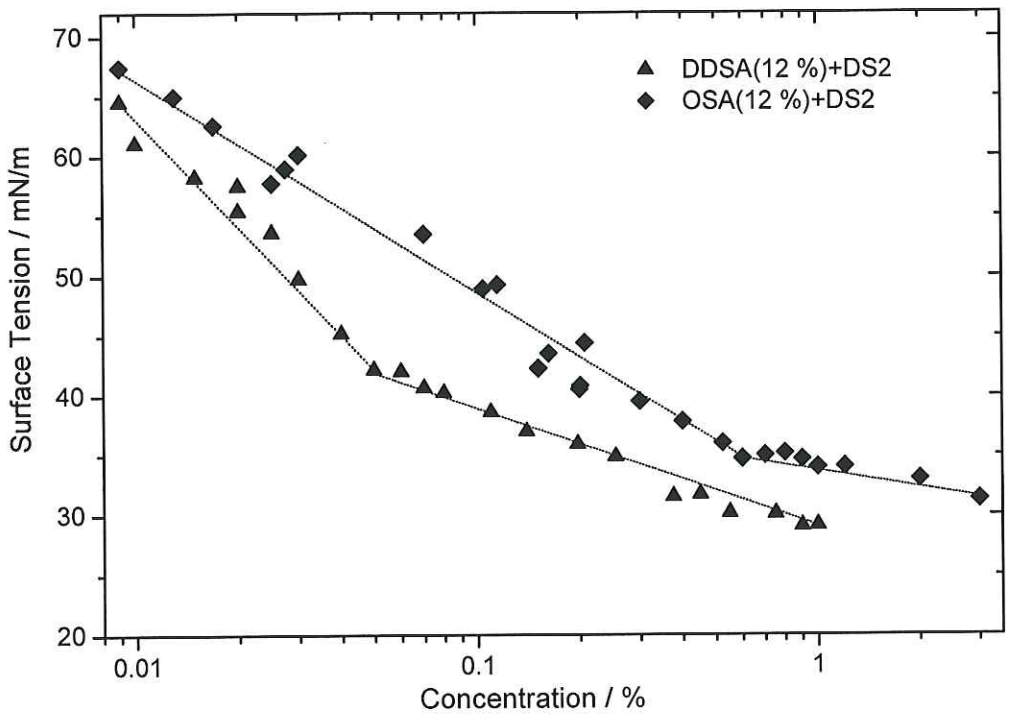

Figure 9. Concentration dependence of the surface tension of DDSA (12 %)-inulin and OSA (12 %)-inulin samples as a function of concentration.

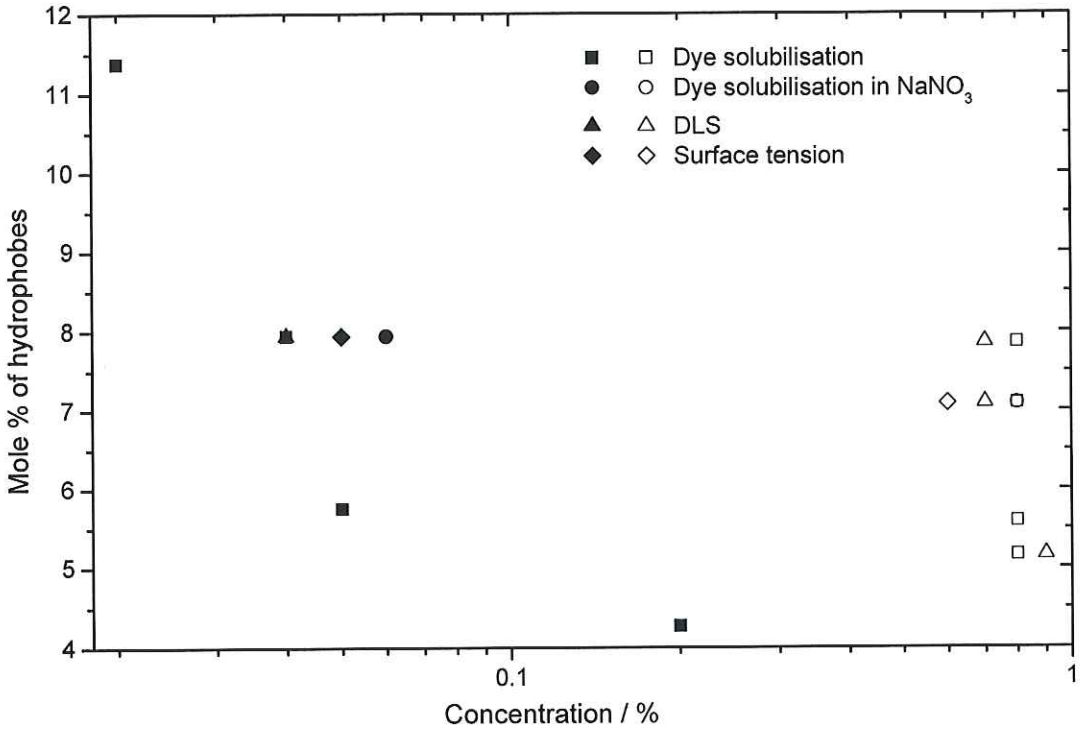

Figure 10. Comparison of the CAC values for ASA-inulin samples with varying % hydrophobe incorporation using dye solubilisation, dynamic light scattering and surface tension measurements.

Table 1. Effect of ASA concentrations on the DS and reaction efficiencies of ASA-inulins.

Sample	% substitution / moles	% reaction efficiency
OSA (6 %)+N10	5.16	85
OSA (6 %)+DS2	5.59	93
OSA (9 %)+DS2	7.86	87
OSA (12 %)+DS2	7.09	59
DDSA (6 %)+DS2	4.27	71
DDSA (9 %)+DS2	5.75	64
DDSA (12 %)+DS2	7.94	66
DDSA (12 %)+DS2 at 50 °C	11.38	95

Table 2. Molecular mass and polydispersity of the inulin and ASA-inulin samples.

Sample	M_w (g/mol)	M_n (g/mol)	M_w/M_n
Native inulin Fibruline® DS2 0.80 %	3.76E+03	3.00E+03	1.252
OSA(12 %)+DS2 0.20 %	4.04E+03	3.45E+03	1.171
OSA(12 %)+DS2 0.40 %	4.09E+03	3.30E+03	1.247
OSA(12 %)+DS2 1.00 %	5.46E+03	4.61E+03	1.186
DDSA (12 %)+DS2 0.40 %	6.61E+03	4.57E+03	1.485
DDSA (12 %)+DS2 0.8 %	7.40E+03	5.65E+03	1.310

Table 3. Critical aggregation concentrations of the ASA-inulin samples using various techniques.

Samples	%			
	Dye solubilisation		DLS	Surface tension
	in water	in 0.1M $NaNO_3$	in water	in water
OSA(6%)+DS2	0.8		~0.9	
OSA(6%)+N10	0.8			
OSA(9%)+DS2	0.8		~0.7	
OSA(12%)+DS2	0.8	0.8	~0.7	0.6
DDSA(6%)+DS2	0.2			
DDSA(9%)+DS2	0.05			
DDSA(12%)+DS2	0.04	0.06	0.04	0.05
DDSA(12%)+DS2 at 50 °C	0.02			